Otology & Neurotology
33:328–334 © 2012, Otology & Neurotology, Inc.

Comparison of Cochlear Implant Relevant Anatomy in Children Versus Adults

*Theodore R. McRackan, †Fitsum A. Reda, *Alejandro Rivas, †Jack H. Noble, *Mary S. Dietrich, †Benoit M. Dawant, and *Robert F. Labadie

**Department of Otolaryngology–Head and Neck Surgery, Vanderbilt University Medical Center; and †Electrical Engineering and Computer Science, Vanderbilt University, Nashville, Tennessee, U.S.A.*

Hypothesis: To test whether there are significant differences in pediatric and adult temporal bone anatomy as related to cochlear implant (CI) surgery.
Background: Surgeons rely upon anatomic landmarks including the round window (RW) and facial recess (FR) to place CI electrodes within the scala tympani. Anecdotally, clinicians report differences in orientation of such structures in children versus adults.
Methods: Institutional review board approval was obtained. High-resolution computed tomographic scans of 24 pediatric patients (46 ears) and 20 adult patients (40 ears) were evaluated using software consisting of a model-based segmentation algorithm that automatically localizes and segments temporal bone anatomy (e.g., facial nerve, chorda tympani, external auditory canal [EAC], and cochlea). On these scans, angles pertinent anatomy were manually delineated and measured blinded as to the age of the patient.
Results: The EAC and FR were more parallel to the basal turn (BT) of the cochlea in children versus adults (∠ EAC:BT 20.55 degrees versus 24.28 degrees, $p = 0.003$; ∠FR:BT 5.15degrees versus 6.88 degrees, $p = 0.009$). The RW was more closely aligned with the FR in children versus adults (∠FR:RW 30.43 degrees versus 36.67 degrees, $p = 0.009$). Comparing the lateral portion of the EAC (using LatEAC as a marker) to the most medial portion (using ⊥TM as a marker), the measured angle was 136.57 degrees in children and 172.20 degrees in adults ($p < 0.001$).
Conclusion: There are significant differences in the temporal bone anatomy of children versus adults pertinent to CI electrode insertion. **Key Words:** Cochlear implants—Pediatric cochlear implantation—Temporal bone anatomy.

Otol Neurotol **33:**328–334, 2012.

The frequency of cochlear implantation (CI) in the pediatric population has increased dramatically since the early 1990s. Although many surgeons feel that CI can be more difficult in the pediatric population as compared with adults, there is little evidence to support why this may be the case.

Although embryologic growth of the temporal bone is fairly well understood, postnatal temporal bone growth is more highly debated. Historically, it was believed that the morphology and spatial orientation of the labyrinth did not change significantly after birth (1,2). It now seems that the cranium undergoes a bimodal growth curve occurring at ages 1 to 4 and then again during puberty, which may have significant impact on temporal bone anatomy (3,4). It has been suggested that these changes occur in the mastoid process and tympanic and squamous portions of the temporal bone rather than in the bony labyrinth (4).

With regard to CI relevant anatomy, the width of the facial recess (FR) does not seem to be significantly different in children and adults (5–8). Furthermore, there also does not seem to be differences in FR width in children younger than one year compared with those 2 to 3 years old (5). However, there is some evidence to show that the basal turn of the cochlea may change orientation with respect to the FR as an individual grows (9).

Although changes in one structure can alter a surgeon's view, it is more often the relationship of multiple anatomic sites that can affect the ease or difficulty of surgery. Herein, we discuss the important anatomic relationships for CI surgery and how these relationships differ in children compared with adults.

Address correspondence and reprint requests to Robert F. Labadie, M.D., Ph.D., 10265 Medical Center East, South Tower Vanderbilt University Medical Center, Nashville, TN 37232-8606; E-mail: robert.labadie@vanderbilt.edu

This manuscript is to be presented at the American Neurotology Society Meeting in Chicago, IL (4/11).

The project described was supported by Award Number R01 DC008408 and R01 DC010184 from the National Institute on Deafness and Other Communication Disorders. The content is solely the responsibility of the authors and does not necessarily represent the official views of the National Institute on Deafness and Other Communication Disorders or the National Institutes of Health.

The authors disclose no other conflicts of interest.

METHODS

Subjects

Institutional review board approval was obtained. The preoperative computed tomographic (CT) scans of patients undergoing CI were evaluated. Patients with cochlear malformations (e.g., common cavity, Mondini malformation) were excluded from this study. Each ear was treated as an independent variable in statistical analysis.

CT Scans

In constructing the models for the segmentation of the temporal bone anatomies, we used image volumes acquired from several scanners, including Philips Mx8000 IDT 16, Siemens Sensation Cardiac 64, and Philips Brilliance 64. The scans were acquired at 120 to 140 KVp and exposure times 265 to 1,000 mA s. Typical scan resolution is 512 × 512 × 130 voxels for pediatric and 768 × 768 × 300 voxels for adult scans with typical voxel size of 0.3 × 0.3 × 0.4 mm.

Automatic Segmentation of Anatomic Structures

The ear canal, tympanic membrane, scala tympani, scala vestibuli, ossicles, facial nerve, chorda tympani, and the cochlea were automatically segmented in the CT images with a series of previously published algorithms (10–15). Although the detailed description of this is beyond the scope of the current article, these techniques rely on reference CT volumes, which are called atlases. For these atlases, models have been created using the manual delineation of structures of interest in a number of CT scans (12 scans for our pediatric model and 15 scans for our adult model). To segment a new image volume, the atlases are spatially aligned with the new image using automatic registration techniques; the models are projected from the atlases to the new volume and automatically adjusted to precisely localize the structures of interest in this image volume using image intensity information.

After performing both intensity-based rigid registration—in which the atlas is rotated and translated to match the unknown CT scan—and intensity-based nonrigid registration—in which the images are stretched, the external auditory canal (EAC), tympanic membrane (TM), ossicles, external boundary of the cochlea, and bone-encased regions of the FN (i.e., at the mastoid tip and at the second genu) are accurately identified. To delineate the course of the FN and the chorda tympani (ChT), an additional algorithm is necessary, which we term the NOMAD algorithm for navigated optimal medial axis and deformable model algorithm (10). The NOMAD algorithm was designed for segmenting tubular structures and begins with start and stop points for such structures, which have been identified via the initial rigid and nonrigid registration. Starting with the facial nerve at the mastoid tip as a starting point, the algorithm analyzes each neighboring voxel and, based upon intensity and expected orientation, progresses through the image until the end point (second genu) is reached. In selecting which voxel to move to next, the algorithm uses information gathered from the models and determines the path in the images that matches best expected intensity values and direction at each point. This algorithm produces a central line for the FN and ChT. The complete structure is identified with a level set–based algorithm that expands the centerline (16). The expansion of the centerline is guided by a priori information on structure diameter stored in the model and by the intensity values in the images; for example, the algorithm stops where there is an edge in the image.

For the precise localization of the intracochlear anatomy, that is, the scala tympani (ST) and scala vestibuli (SV), we use what is called a statistical shape model (17). We built these models using μCT scans (Scanco μCT scanner, voxel size 36 μm isotropic) of 6 cadaveric human cochleae in which the outline of ST and SV were manually delineated. These models capture anatomic variability in intracochlear structures and permit localizing the position of structure boundaries based on incomplete information, for example, the position of the ST and of the SV can

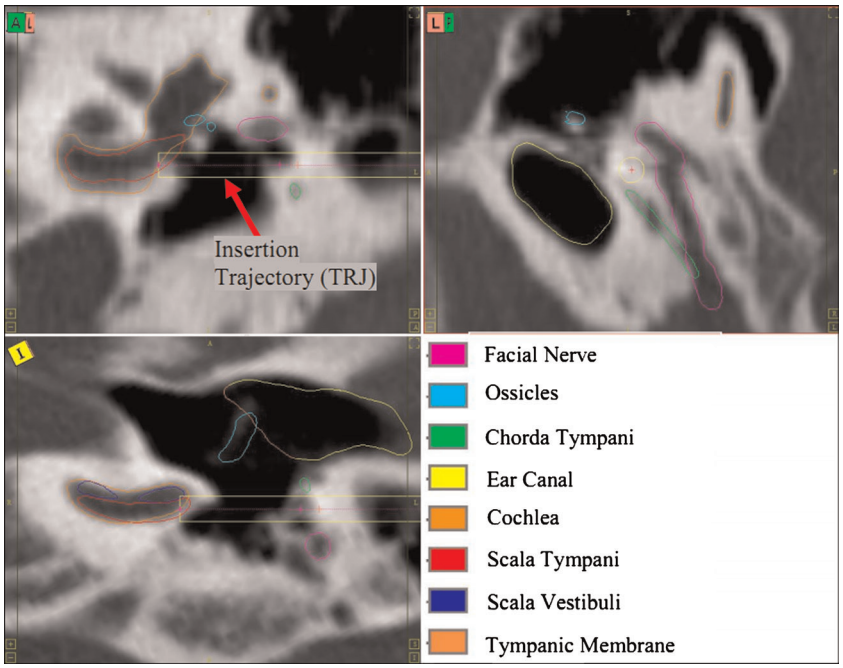

FIG. 1. Contours of the temporal bone anatomy and trajectory computed using these segmentations.

be inferred from the position of the external boundary of the cochlea. Published work has shown the accuracy and reliability of these methods (10,11,14). An example of segmentation results are seen in Figure 1.

Determination of Anatomic Relationships

To compare the orientations of the structures, the following lines were computed with no regard to the patient's age (Fig. 2):

1. Drilling trajectory line (TRJ)—This line was computed using a method we have developed for computing an optimally safe trajectory for CI insertion that passes through the facial recess and through the round window (RW) into the scala tympani (12).
2. Most lateral ear canal center line (LatEAC)—The start and end of the most lateral region of the bony ear canal were manually delineated. The start point is defined as the center of the most external portion of the ear canal and the second point as the center of the region of the ear canal just before the ear drum intersects it. As a result, a set of 3-dimensional points were produced in the reference volume. The 3-dimensional points were then projected onto each subject CT scan. Finally, the centers of mass of the projected points were used to mark the start and end points of the LatEAC line.
3. Line perpendicular to tympanic membrane (TM) plane (⊥TM)—The TM surface was manually segmented in the reference volume. Then, points on the TM surface were projected onto each subject CT scan. A plane was subsequently fitted to the projected points to define the tympanic plane (TP) in each subject CT scan. Finally, the normal to the TP (⊥TM) that passes through its center, which is defined as the center of mass of the projected points, was computed.
4. Line perpendicular to the RW (⊥RW)—The RW surface was manually delineated in the reference volume. Then, the points on this surface were projected onto each subject CT scan. A plane was fitted to the set of projected points to define the RW plane. Finally, the normal to this plane (⊥RW) that passes through its center, which is defined as the center of mass of the projected points, was computed.
5. Long axis of the basal turn of the cochlea (BT)—The first point was manually localized near the RW at the end of the scala tympani surface, and its location was saved in the reference volume. Next, the central axis of the cochlea was manually determined in the same volume. Then, a second point was localized 180 degrees away from this point also in the reference volume. The angle was measured as follows: 1) a line perpendicular to the central axis was computed from the first point to the central axis, 2) the second point was moved along the centerline of the scala tympani, 3) a line perpendicular to the central axis was computed from the current location of the second point to the central axis, 4) the desired angle was then computed between the lines computed in 1) and in 3). Finally, the 2 points are projected onto each subject CT scan to produce the line of the long axis of the scala tympani.
6. Line perpendicular to the plane that bisects the facial recess (⊥FR)—A plane that passes through the facial recess was defined using 3 points on each subject CT scan. Two of the points that are used in defining the plane are the start and end points of the insertion trajectory. The third point was estimated as the medial point (center of mass) of the region of the lower end of the chorda tympani and facial nerve. Finally, the line perpendicular to the defined plane (⊥FR) that passes through the center of mass of the 3 points was computed.

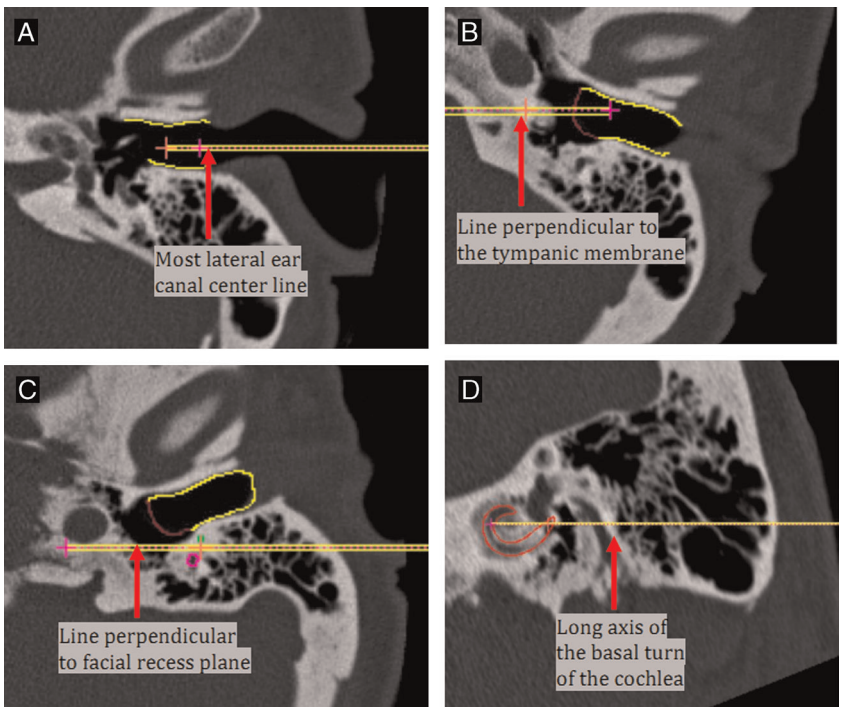

FIG. 2. Examples of vectors identified. (*A*) Most lateral ear canal center line (Lat EAC): EAC is outlined in yellow. (*B*) Line perpendicular to TM (^TM): gain EAC is yellow and TM is outlined in red. (*C*) Line perpendicular to facial recess plane (^FR): facial nerve is outline in pink; chorda tympani is outlined in green. (*D*) Long axis of the basal turn of the cochlea (BT): scala tympani is outlined in red.

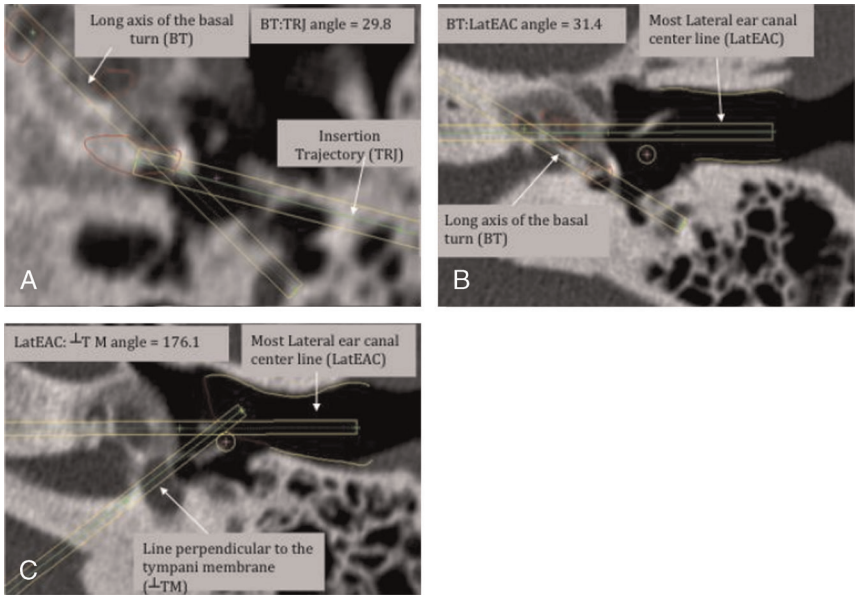

FIG. 3. Comparison of BT and TRJ (*A*, scala tympani in red), comparison of BT and LatEAC (*B*, scala tympani in red; lateral EAC in yellow), and comparison of LatEAC and line perpendicular to TM (*C*, TM in red; EAC in yellow).

The angles between the lines were used as features. These are obtained by computing the arc cosine of the normalized dot product of the lines (vectors). Although labeling is difficult in 2-dimensional radiographs, Figure 3 provides examples of the angles compared for this paper.

Statistical Methods

Comparisons between the pediatric and adult samples were conducted using mixed effects linear modeling analysis that included the ear within the patient as a random effect. The distributions of the angle values were evaluated for normality before conducting tests of statistical significance. Some values were severely skewed and were rank transformed for appropriate use of the mixed effects linear modeling approach. Associations of age with the angle measures within each patient group were conducted using Spearman rank correlations.

RESULTS

In total, 46 pediatric ears (23 patients) and 40 adult ears (20 patients) were analyzed. The pediatric and adult

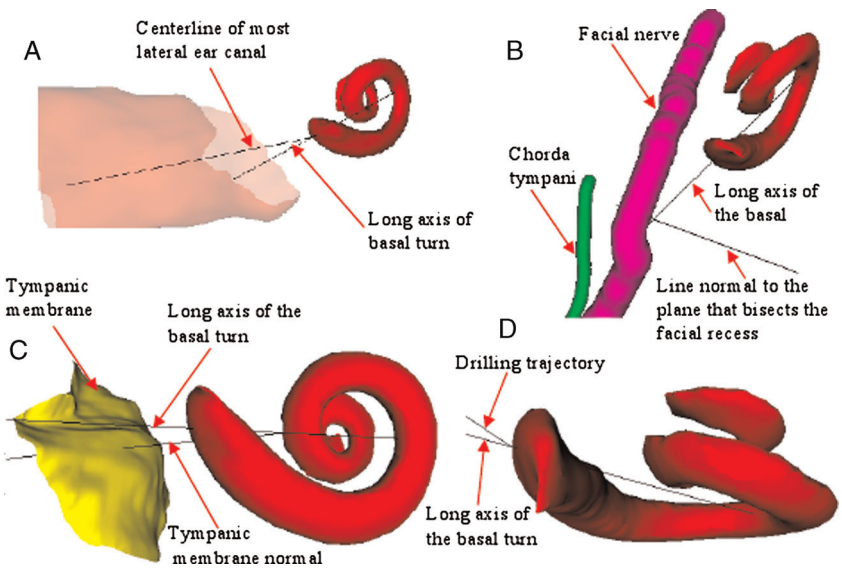

FIG. 4. Orientation about the long axis of the basal turn of the cochlea. Demonstration of the angle between the following: *(A)* the center line of the most lateral ear canal (LatEAC) and the long axis of the basal turn of the cochlea (BT), (*B*) line perpendicular to the facial recess (⊥1-FR) and the long axis of the basal turn of the cochlea (ET) (purple, facial nerve; green, chorda tympani); (*C*) line perpendicular to the tympanic membrane (⊥1-TM) and the long axis of the basal turn of the cochlea (BT); (*D*) the selected drilling trajectory (TRJ) and the long axis of the basal turn of the cochlea (BT).

TABLE 1. *Comparison of relationship about the long axis of the basal turn of the cochlea*

Relationship	Average pediatric angle (SD)	Average adult angle (SD)	*p*
BT:LatEAC	20.55 (0.82)	24.28 (0.88)	0.003
BT:⊥FR	5.15 (0.62)	6.88 (0.66)	0.009
BT:⊥TM	53.96 (0.94)	31.47 (1.01)	<0.001
BT:TRJ	32.56 (1.98)	21.90 (2.13)	<0.001

BT indicates long axis of the basal turn of the cochlea; ⊥FR, line perpendicular to the facial recess; LatEAC, center line of the external auditory canal; SD, standard deviation; ⊥TM, line perpendicular to the tympanic membrane; TRJ, ideal drilling trajectory for cochleostomy.

TABLE 2. *Comparison of relationships about the lateral most portion of the external auditory canal*

Relationship	Average pediatric angle (SD)	Average adult angle (SD)	*p*
LatEAC:⊥TM	136.57 (1.08)	172.20 (1.15)	0.003
LatEAC:⊥RW	43.41 (1.09)	52.34 (1.17)	0.009
LatEAC:⊥FR	10.06 (0.81)	14.42 (0.87)	<0.001
LatEAC:TRJ	23.51 (2.47)	19.40 (2.65)	<0.001

⊥RW indicates line perpendicular to the plane of the round window.

median ages were 3.0 (range, 0.8–16 yr) and 53.0 years (range, 30–75 yr), respectively.

Orientation About BT of the Cochlea

Orientation about the BT was chosen as it represents the target for CI electrode placement. Two of the major visual hurdles for CI are the relationships between the RW and the EAC and the RW and the FR. In this study, the BT serves as a marker for RW and cochlear orientation, whereas the LatEAC and ⊥FR are markers for the axis of the EAC and FR, respectively (Fig. 4). In comparing the angles between these structures in children versus adults, there was a clear statistical difference observed (Table 1). The average angle between BT and LatEAC (∠BT:EAC) was 20.55 degrees in children and 24.28 degrees in adults ($p = 0.003$), and the ∠BT:⊥FR was 5.15 degrees in children and 6.88 degrees in adults ($p = 0.009$) (Table 1). Because there is difference in EAC orientation in children and adults (described later), we also measured the angle of the more medial portion of the EAC (⊥TM) and the BT. Similar to LatEAC, the difference in BT:⊥TM orientation was statistically significant

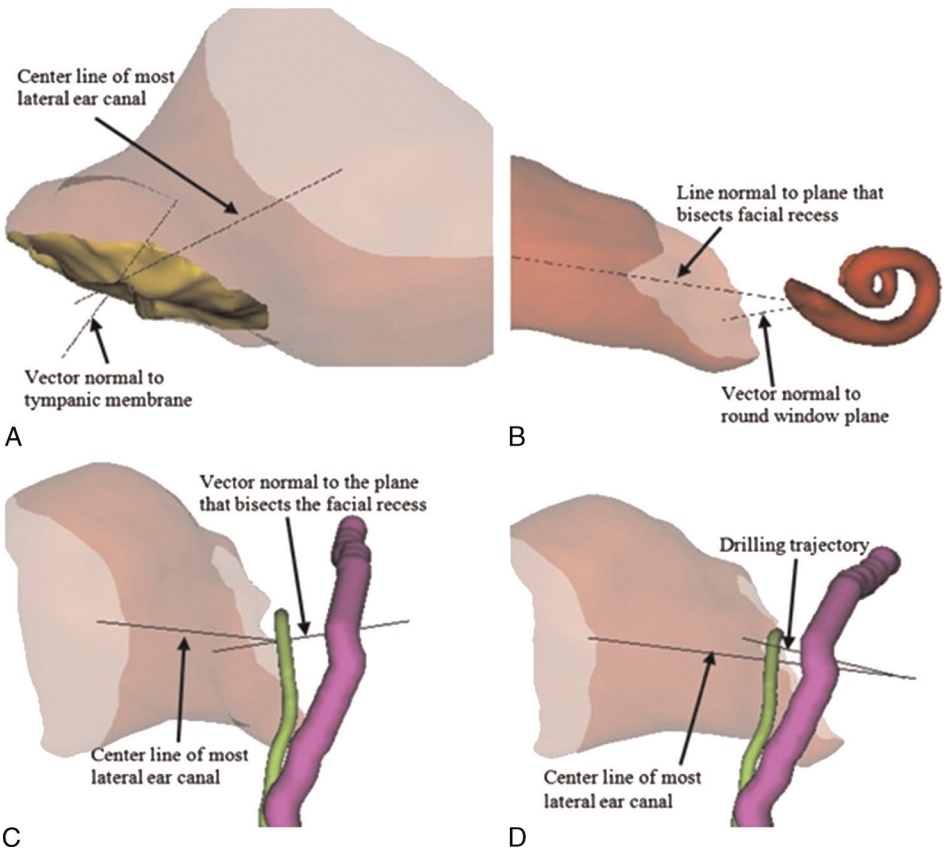

FIG. 5. Orientation about the center line of the lateral most portion of the EAC. Demonstration of the angle between the following: (*A*) line perpendicular to the TM (⊥TM) and the center line of the lateral most portion of the EAC (LatEAC); (*B*) line perpendicular to the round window plane (⊥RW) and the center line of the lateral most portion of the EAC (LatEAC); (*C*) line perpendicular to the plane of the facial recess and the center line of the lateral most portion of the EAC (LatEAC); (*D*) the drilling trajectory line (TRJ) and the center line of the lateral most portion of the EAC (LatEAC) (purple, facial nerve; green, chorda tympani).

(53.96 degrees in children versus 31.47 degrees in adults; $p < 0.001$). There also was a statistically significant difference when comparing the selected ideal drilling trajectory for scala tympani electrode insertion to the BT (32.56 degrees children versus 21.90 degrees adults; $p < 0.001$).

Orientation About the Centerline of the Lateral Most Portion of the EAC

In anecdotal reports, the lateral portion of the EAC in children can be a substantial impediment to the visualization necessary for CI. Indeed, there does appear to be statistical differences in EAC orientation in children compared with adults (Fig. 5; Table 2). When comparing the lateral portion of the EAC (using LatEAC as a marker) to the most medial portion (using ⊥TM as a marker), the measured angle in children was 136.57 and 172.20 degrees in adults ($p < 0.003$).

We then compared the LatEAC with other important anatomic sites important for CI (Table 2). With regard to RW visualization, the angle between Lat EAC and a plane perpendicular to the RW (∠LatEAC:⊥RW) was 43.41 degrees in children and 52.34 in adults ($p < 0.009$). The difference in orientation of LatEAC and the plane perpendicular to the (⊥FR) was statistically significant (10.06 degrees in children and 14.42 degrees in adults; $p = 0.01$) as was the difference in LatEAC and TRJ orientation (23.51 degrees in children and 19.40 degrees in adult; $p = 0.001$).

Orientation About the RW

We chose to use a vector perpendicular to the RW plane (⊥RW) as a marker for RW orientation (Fig. 6). In comparing the relationship between ⊥RW and the ideal drilling trajectory (TRJ), we found no statistically significant difference between children and adults (41.39 degrees versus 39.47 degrees; $p = 0.003$; Table 3). However, when evaluating the differences in orientation between ⊥RW and ⊥FR, there was a statistically significant difference (30.43 degrees in children versus 36.67 degrees in adults; $p < 0.009$).

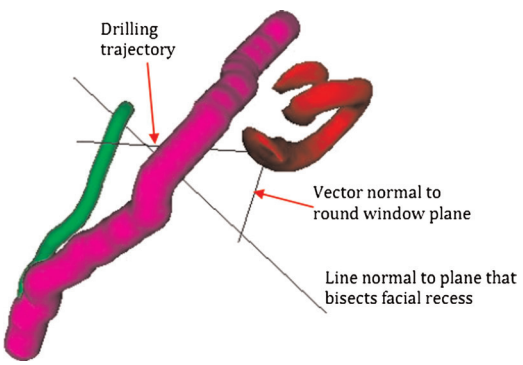

FIG. 6. Orientation about the RW. Demonstration of the angle between the optimal drilling trajectory (TRJ) and the line perpendicular to the RW (⊥LRW) as well as the line perpendicular to the facial recess plane and the line perpendicular to the RW (⊥RW).

TABLE 3. *Comparison of relationships about the round window*

Relationship	Average pediatric angle (SD)	Average adult angle (SD)	*p*
⊥RW:TRJ	41.39 (1.30)	39.47 (1.39)	0.003
⊥RW:⊥FR	30.43 (0.94)	36.67 (1.00)	0.009

SD indicates standard deviation; ⊥RW, line perpendicular to the plane of the round window; ⊥FR, line perpendicular to the facial recess; TRJ, ideal drilling trajectory for cochleostomy.

DISCUSSION

Data pertaining to changes in cochlear orientation with increasing age are sparse, with multiple sources stating that no such changes occur (1,2). Although this paper does not deal directly with single anatomic site variation with age, it does display significant changes in relationships in temporal bone anatomy relevant to CI. These orientations are important in otologic surgery as a surgeon depends heavily on anatomic relationships to estimate anatomy hidden by bone.

Exposure of the Facial Recess

The description of the differences in EAC anatomy in children versus adults is an interesting but not novel finding (5). Although it is well known that the EAC orientation changes from an obtuse angle to more of a straight line, there is no objective data to describe this. We found that angle between the lateral EAC and the more medial EAC was 35.63 degrees more obtuse ($p = 0.003$) in the adult population compared with children (Table 2). The more posterior orientation of the lateral EAC could have significant impact on visualization of the FR and the RW.

With regard to the relationship of the latEAC and the FR, we also found a statistically significant difference in this orientation in children and adults. This angle is more acute in children, meaning that the surgeon has a more narrow view of the FR in the pediatric population; this suggests more difficulty placing CI electrodes via the FR. Based on our data, it is impossible to say whether this result is from changes solely in EAC or FR orientation. However, based on the above data, it is likely because of changes in both as there were significant difference in each orientation with regard to the ideal cochleostomy drilling trajectory and the long axis of the basal turn of the cochlea. This calls into question previous belief of minimal postnatal movement of the vertical segment of the facial nerve (7,18,19).

Exposure of the RW and Cochlea

We found several significant differences with orientation about the RW and the cochlea. The angles between the long axis of the basal turn of the cochlea and the lateral portion of the EAC as well as the angle between the long axis of the basal turn of the cochlea and the plane of the facial recess were statistically more acute in

children compared with adults. Again, these more acute angles describe a narrower view of the RW and possibly increased difficulty with CI.

Conversely, the orientation of the ideal cochleostomy drilling trajectory compared with the long axis of the basal turn of the cochlea is statistically more obtuse in children. From this information, we can infer that there is significant alteration in the facial recess or cochlea orientation as the ideal trajectory is moved more anteriorly in children, making the angle more obtuse. Similarly, the view of the RW through the facial recess is significantly less of a straight line (10.66 degrees more acute) in children, making electrode implantation more difficult. Postnatal alterations in cochlear orientation have been recently described (9), calling into question previous data regarding cochlear stagnancy (19). The report by Lloyd et al. (9) of decreasing basal turn angle with regard to the sagittal plane with age is consistent with the findings in our study.

Drilling Trajectory Comparison

The data comparing the ideal cochleostomy drilling trajectory and the EAC orientation in adults and children are in harmony with above comments where we described how the adult EAC is significantly more obtuse when compared with children. Our data show that the drilling trajectory is significantly closer to paralleling the lateral EAC in adults as compared with children (19.40 degrees versus 23.51 degrees, respectively; $p < 0.001$). This again suggests that the surgeon's view of the RW through the facial recess is less obstructed in adults and more in line with that view.

Although we have identified significant differences in pediatric and adult cochlear implant relevant anatomy, we still do not yet know when such changes occur. Because of the relatively small sample size of this study, there were no statistically significant trends identified. We plan to further investigate when such changes occur using either larger populations of pediatric patients or, ideally, serial scans of pediatric patients. We also recognize that there may be unknown errors in the rigid and non-rigid registration processes in identifying important anatomic structures. Although registration is manually confirmed and, if necessary, adjusted in each case, the accuracy of the verification is limited by the resolution of the imaging study as well as human visual acuity in identifying suboptimal registration. Nonetheless, our data represent a part of a growing body of literature suggesting that differences in labyrinthine anatomy do indeed exist (20–22).

CONCLUSION

It has been widely shown that there are no statistically significant differences in facial recess width in children as compared with adults. However, this does not do justice the differences in anatomic orientation that come into play during pediatric CI surgery. We have shown a number of statistically significant differences in orientation among the EAC, facial recess, RW plane, and the long axis of the basal turn of the cochlea in children and adults that help to explain the difference between adult and pediatric CI.

REFERENCES

1. Bast TH. Development of the otic capsule. VI. Histological changes and variations in the growing bony capsule of the vestibule and cochlea. *Ann Otol Rhinol Laryngol* 1942;51:343–57.
2. Schonemann A. Schlafenbein und Schadelbasis, eine anatomischotiatrische Studie. *N Denkschr algem Schweizer Gesellsch gesamt Naturwiss* 1906;40:95–160.
3. Farkas LG, Posnick JC, Hreczko TM. Anthropometric growth study of the head. *Cleft Palate Craniofac J* 1992;29:303–8.
4. Eby TL. Development of the facial recess: implications for cochlear implantation. *Laryngoscope* 1996;106:1–7.
5. Bielamowicz SA, Coker NJ, Jenkins HA, Igarashi M. Surgical dimensions of the facial recess in adults and children. *Arch Otolaryngol Head Neck Surg* 1988;114:534–7.
6. Eby TL, Nadol JB. Postnatal growth of the human temporal bone: Implications for cochlear implants in children. *Ann Otol Rhinol Laryngol* 1986;95:356–64.
7. Su W-Y, Marion MS, Hinojosa R, et al. Anatomical measurements of the cochlear aqueduct, round window membrane, round window niche, and facial recess. *Laryngoscope* 1982;92:483–6.
8. Bettman RH, Appelman AM, van Olphen AF, et al. Cochlear orientation and dimensions of the facial recess in cochlear implantation. *ORL J Otorhinolaryngol Relat Spec* 2003;65:353–8.
9. Lloyd SKW, Kasbekar AV, Kenway B, et al. Developmental changes in cochlear orientation—implications for cochlear implantation. *Otol Neurotol* 2010;31:902–7.
10. Noble JH, Warren FM, Labadie RF, Dawant BM. Automatic segmentation of the facial nerve and chorda tympani in CT images using a spatially dependent feature values. *Med Phys* 2008;35:5375–84.
11. Reda FA, Noble JH, Rivas A, McRackan TR, Labadie RF, Dawant BM. Automatic segmentation of the facial nerve and chorda tympani in pediatric CT scans. *Med Physics* 2011;38:5590–600.
12. Noble JH, Majdani O, Labadie RF, et al. Automatic determination of optimal linear drilling trajectories for cochlea access accounting for drill-positioning error. *Int J Med Robotics Comput Assist Surg* 2010;6:281–90.
13. Noble JH, Rutherford RB, Labadie RF, Dawant BM. Modeling and segmentation of intra-cochlear anatomy in conventional CT. *IEEE Trans On Biomedical Eng* 2011;58:2625–32.
14. Noble JH, Dawant BM. An atlas-navigated optimal medial axis and deformable model algorithm (NOMAD) for the segmentation of the optic nerves and chiasm in MR and CT images. *Med Image Anal* 2011;15:877–84.
15. Noble JH, Dawant BM, Warren FM, Majdani O, Labadie RF. Automatic identification and 3-D rendering of temporal bone anatomy. *Otol Neurotol* 2009;30:436–42.
16. Sethian J. *Level Set Methods and Fast Marching Methods*, 2nd ed. Cambridge, MA: Cambridge University Press, 1999.
17. Cootes TF, Taylor CJ, Cooper DH, et al. Active shape models—their training and application. *Comp Vis Image Unders* 1995;61:39–59.
18. Litton WB, Krause CJ, Anson BA, et al. The relationship of the facial canal to the annular sulcus. *Laryngoscope* 1969;79:1584–604.
19. Jeffery N, Spoor F. Prenatal growth and development of the modern human labyrinth. *J Anat* 2004;204:71–92.
20. Martinez-Monedero R, Niparko JK, Aygun N. Cochlear coiling pattern and orientation differences in cochlear implant candidates. *Otol Neurotol* 2011;32:1086–93.
21. Verbist BM, Joemai RM, Briaire JJ, Teeuwisse WM, Veldkamp WJ, Frijns JH. Cochlear coordinates in regard to cochlear implantation: a clinically individually applicable 3 dimensional CT-based method. *Otol Neurotol* 2010;31:738–44.
22. Erixon E, Högstorp H, Wadin K, Rask-Andersen H. Variational anatomy of the human cochlea: implications for cochlear implantation. *Otol Neurotol* 2009;30:14–22.